Progress In Electromagnetics Research B, Vol. 44, 31–52, 2012

INVESTIGATION OF DIFFERENT BASIS AND TESTING FUNCTIONS IN METHOD OF MOMENTS FOR ELECTROSTATIC PROBLEMS

R. H. Alad[1, *] and S. B. Chakrabarty[2]

[1]Department of Electronics and Communication, Faculty of Technology, Dharmsinh Desai University, Nadiad, Gujarat, India

[2]Antenna Systems Group, Space Applications Centre, Ahmedabad, Gujarat, India

Abstract—This paper presents comparative studies on different types of basis and testing functions used in Method of Moments (MoM) in terms of analytical complexity, convergence and condition number of the co-efficient matrix when applied to electrostatic problem of evaluating capacitance and charge distribution of conducting bodies. A thin conducting cylinder of finite length has been taken as a representative case study to evaluate the capacitance and charge distribution. The basis and testing functions which have been studied for this problem are pulse-delta, pulse-pulse, triangular-delta, triangular-pulse and triangular-triangular functions respectively. Numerical data on capacitance and charge distribution has been presented for each set of basis and testing functions in terms of condition number and convergence.

1. INTRODUCTION

Method of Moments has been widely used for the solution of a large class of electromagnetic problems including electrostatic problems during the last few decades. Harrington [1] presented the computation of capacitance and charge distribution of a conducting square plate and a cylinder using the method of moments based on pulse function as basis function and delta functions as testing functions. In view of the importance of electrostatic modeling of space-craft bodies for the studies of electrostatic discharges (ESD) problems, the capacitance and charge distribution of metallic structures in the form of a conducting

Received 6 July 2012, Accepted 7 September 2012, Scheduled 16 September 2012

* Corresponding author: Rizwan Habibbhai Alad (rizwan_alad@yahoo.com).

cylinder of finite axial length, truncated cone, rectangular plates, paraboloidal, spherical reflectors etc. were analyzed using MoM [2–8]. Electrostatic modeling of dielectric coated metallic bodies based on MoM has also been reported [9–11]. In all the works, pulse function as basis function and delta function as testing function were used as suggested by Harrington [1] for solving the integral equations relating to unknown charge to a known potential. The choice of basis and testing functions mainly depend on the accuracy of desired solution, the ease of evaluation of the matrix elements, size of the set of simultaneous equations that can be solved by matrix method and the formation of a well-conditioned matrix [12, 13]. There may be a number of sets of basis and testing functions that may be selected for a particular type of problem, some sets may give faster convergence than others, or give easier evaluation of matrix, or give acceptable results with smaller matrix size etc.. The choice of pulse function as basis function and delta function as testing functions as reported by Harrington [1] and subsequently by others [2–8] makes easier evaluation of matrix elements, however, the convergence is very slow and in order to achieve higher accuracy, the numbers of sections have to be increased and sometimes the matrix becomes ill-conditioned. The other limitation of this set of basis and testing functions is that when the observation and source points are the same representing the diagonal elements, the integrand becomes singular and thus the diagonal elements have to be treated separately. Thus, it is worthwhile to carry out analysis using different sets of basis and testing functions to evolve more efficient computation of electrostatic problems and to the best of authors' knowledge, this has not been reported in open literature.

In this article, studies on different basis functions as well as testing functions have been carried out in terms of matrix size for faster convergence. The geometrical configuration which has been considered is a charged conducting cylinder. This paper is organized as follows: Section 2 presents the analysis of a charged conducting cylinder of finite length using different basis and testing functions like pulse/delta, pulse/pulse, triangle/delta, triangle/pulse, triangle/triangle etc.. Section 3 presents illustrative numerical results and Section 4 presents the summary and discussion.

2. ANALYSIS

Figure 1 shows a circular cylindrical conductor of finite length 'L' and radius 'a'. The potential at position vector $\mathbf{r}$ due to any charge

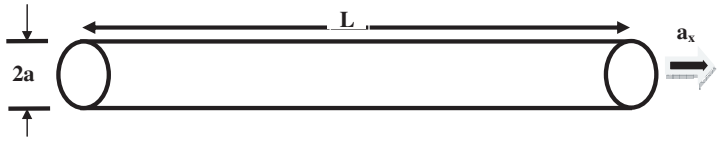

Figure 1. Charged conducting cylinder.

distribution on the cylinder at position vector $\mathbf{r}'$ is given by

$$\Phi(x) = \int\limits_{\Omega} \frac{q_e(x')}{4\pi\varepsilon\,|\mathbf{r}-\mathbf{r}'|}\,d\,\Omega \tag{1}$$

where Ω represents the source region.

In order to find the capacitance of conducting cylinder as shown in Fig. 1, the knowledge of total unknown charge distribution on the metallic surface and the value of potential should be known. Assuming a known potential V, the unknown charge distributions appearing in Eq. (1) expressed in terms of known basis functions [1] as

$$q_e(x') = \sum_{n=1}^{N} \alpha_n f_n \tag{2}$$

where f_n's are the known basis functions α_n's are unknown coefficients to be determined. Substitution of Eq. (2) into (1), yields,

$$\Phi(x) = \int\limits_{\Omega} \sum_{n=1}^{N} \alpha_n f_n * \frac{B\,(x'-x)}{4\pi\varepsilon\,|\mathbf{r}-\mathbf{r}'|}\,d\,\Omega \tag{3}$$

Considering, the source points are on the cylinder axis and observation points on the surface of the cylinder, the above problem is posed to one-dimensional problem. The localized nature of basis functions $B(x'-x)$ restricts this integral to be over the nth segment. Local weighted average is formed about each point $x_m = m\Delta$ by using another local weighting (or testing) function $W(x-x_m)$, which is centred on x_m and (3) may be rewritten as,

$$4\pi\varepsilon \int\limits_{(m-1)\Delta x}^{m\Delta x} W\left(x-x'\right) V(x)dx$$

$$= \sum_{n=1}^{N} \alpha_n \int\limits_{(n-1)\Delta x}^{n\Delta x} \int\limits_{(m-1)\Delta x}^{m\Delta x} \frac{W(x-x_n) * B(x'-x)}{\sqrt{(x-x')^2+a^2}}\,dxdx', \quad m = 1, \ldots N \tag{4}$$

Eq. (4) may be written in the N X N matrix form as follows:

$$[L]\{\alpha\} = \{V\} \qquad \{\alpha\} = [L]^{-1}\{V\}$$
$$q_e = \sum_{n=1}^{N} \alpha_n \Delta x \qquad C = \frac{q_e}{V} \tag{5}$$

where,

$$L_{mn} = \int_{(n-1)\Delta x}^{n\Delta x} \int_{(m-1)\Delta x}^{m\Delta x} \frac{W(x-x') * B(x'-x)}{\sqrt{(x-x')^2+a^2}}\, dx dx', \qquad m = 1, \ldots, N$$
$$V_m = 4\pi\varepsilon \int_{(m-1)\Delta x}^{m\Delta x} W(x-x')V(x)dx, \qquad m = 1, \ldots, N \tag{6}$$
$$W(x-x') = \partial(x-x'), \qquad \text{Point Matching}$$
$$W(x-x') = B(x-x'), \qquad \text{Galerkin Method}$$

In succeeding sections, the steps followed above will be considered using the following sets of basis and testing functions:

- Pulse-function as basis function and delta function as weighting function (point matching).
- Pulse-function as basis function as well as weighting function (Galerkin weighting).
- Triangular function as basis function with point matching.
- Triangular function as basis function and pulse function as weighting function.
- Triangular basis function with Galerkin weighting.

2.1. Pulse Function as Basis and Delta Function as Testing Function

The conducting cylinder of Fig. 1 is divided into N points with $N-1$ sub-sections as shown in Fig. 2. The pulse basis function is defined as

$$B_n(x) = 1, \qquad x_n \le x \le x_{n+1}$$
$$B_n(x) = 0, \qquad \text{elsewhere} \tag{7}$$

In the case of pulse basis functions and delta testing functions, the matrix elements L_{mn}, given by Eq. (6) is of the form as:

$$L_{mn} = \int_{(n-1)\Delta x}^{n\Delta x} \frac{1}{\sqrt{(x_m - x')^2 + a^2}}\, dx' \tag{8}$$

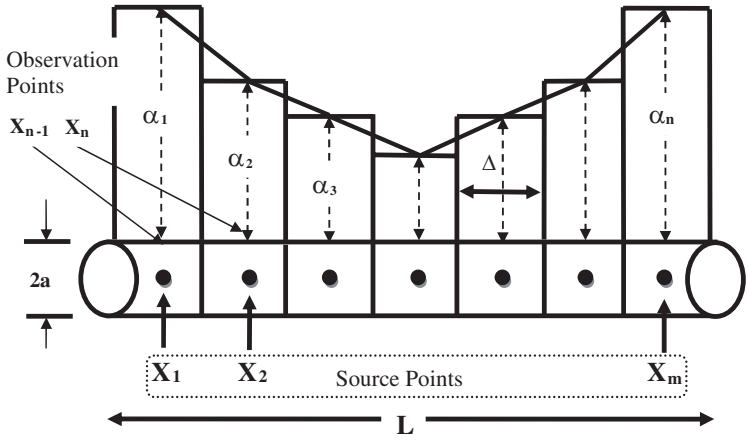

Figure 2. Charged conducting cylinder segmentation with pulse basis & delta weighting function.

After carrying out the integration as in Eq. (8), the following expression is obtained:

$$L_{mn} = \log\left[\frac{(x_{n+1}-x_m)+\sqrt{(x_{n+1}-x_m)^2-a^2}}{(x_{n-1}-x_m)+\sqrt{(x_{n-1}-x_m)^2-a^2}}\right],$$

$$\text{where } x_{n+1} = x_n + \frac{\Delta}{2}, \qquad x_{n-1} = x_n - \frac{\Delta}{2}$$

$$\text{Potential, } V_m = 4\pi\varepsilon \int_{(m-1)\Delta x}^{m\Delta x} \delta\left(x'-x\right) V(x)dx = 4\pi\varepsilon V \quad (9)$$

From Eq. (5), the matrix equation is of the form as given below

$$[L_{mn}]\{\alpha_n\} = \{V_m\} \qquad \{\alpha_n\} = [L_{mn}]^{-1}\{V_m\} \quad (10)$$

The total charge and capacitance of cylinder

$$q_e = \sum_{n=1}^{N} \alpha_n \Delta x \qquad C = \frac{q_e}{V} \quad (11)$$

2.2. Pulse Function as Basis Function with Galerkin Weighting

Using Galerkin's method, with the choice of basis and testing functions both as a pulse function, Eq. (6) may be used to evaluate matrix

elements L_{mn}, as given by

$$L_{mn} = \int_{(n-1)\Delta x}^{n\Delta x} \int_{(m-1)\Delta x}^{m\Delta x} \frac{B\left(x'-x\right) * B\left(x'-x\right)}{\sqrt{(x-x')^2+a^2}} dx dx'$$

$$V_m = 4\pi\varepsilon * \int_{(m-1)\Delta x}^{\Delta x} B\left(x'-x\right) V(x) dx \tag{12}$$

After performing the integration of Eq. (12), the expression for the matrix element is obtained as follows

$$\begin{aligned} L_{mn} = & \sqrt{(x_{m+1}-x_{n+1})^2-a^2}+(x_{m+1}-x_{n+1}) \\ & * \log\left(\sqrt{(x_{m+1}-x_{n+1})^2-a^2}-x_{m+1}+x_{n+1}\right) \\ & -\sqrt{(x_m-x_{n+1})^2-a^2}-(x_m-x_{n+1}) \\ & * \log\left(\sqrt{(x_m-x_{n+1})^2-a^2}-x_m+x_{n+1}\right) \\ & -\sqrt{(x_{m+1}-x_{n-1})^2-a^2}-(x_{m+1}-x_{n-1}) \\ & * \log\left(\sqrt{(x_{m+1}-x_{n-1})^2-a^2}-x_{m+1}+x_{n-1}\right) \\ & +\sqrt{(x_{m-1}-x_{n-1})^2-a^2}+(x_{m-1}-x_{n-1}) \\ & * \log\left(\sqrt{(x_{m-1}-x_{n-1})^2-a^2}-x_{m-1}+x_{n-1}\right), \\ & \text{where} \quad x_{n+1} = x_n + \frac{\Delta}{2}, \qquad x_{n-1} = x_n - \frac{\Delta}{2} \\ & \& \quad x_{m+1} = x_m + \frac{\Delta}{2}, \quad x_{m-1} = x_m - \frac{\Delta}{2} \end{aligned} \tag{13}$$

Also from Eq. (12), the elements of the column matrix are found as follows:

$$V_m = 4\pi\varepsilon * \Delta * V \tag{14}$$

Substituting Eqs. (13) & (14) into Eq. (10) and performing the matrix operation, the unknown charge on each segments are found. Finally using Eq. (11), the total charge on the cylinder and capacitance of the cylinder are computed.

2.3. Triangular Function as Basis Function and Point Matching

A triangle function spans over two segments and varies from zero at the corner points of the segment to unity at the centre point of the

segment. Here, the functions overlap by one segment, hence triangles provide a piecewise linear variation of the solution between segments. A triangle function is defined as

$$\begin{aligned} B_n(x) &= \frac{x - x_{n-1}}{x_n - x_{n-1}}, \qquad x_{n-1} \le x \le x_n \\ B_n(x) &= \frac{x_{n+1} - x}{x_{n+1} - x_n}, \qquad x_n \le x \le x_{n+1} \end{aligned} \tag{15}$$

For the triangular basis, the charge density expansion (Eq. (2)), reads

$$q_e(x') = \sum_{n=1}^{MN} \alpha_n B(x' - x_m),$$
$$B(x' - x_m) \text{ — Basis Function defined in Eq. (15)} \tag{16}$$

The charge distribution along the conducting cylinder for triangular basis functions, depicted in Fig. 3, have span of 2Δ, that is twice as long as the pulse case.

The charged conducting cylinder is divided into N segments of width $\Delta = L/N$ and $N + 1$ points $x_m = m\Delta$, lie at the end points of these segments as shown in Fig. 3. In order to satisfy the condition that the charge density shoots up at the edges, the basis function at the first and last segments has to be a half triangle as illustrated in Fig. 3.

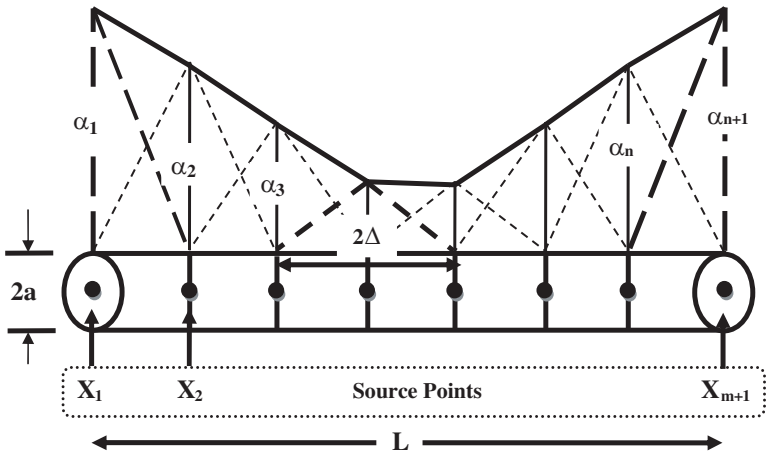

Figure 3. Charged conducting cylinder segmentation with triangular basis & delta weighting function.

For point matching, the equation of matrix elements (6) is of the form:

$$L_{mn} = \int_{x_{n-1}}^{x_n} \left(\frac{x' - x_{n-1}}{\Delta} \right) * \frac{1}{\sqrt{(x_m - x')^2 + a^2}} \, dx' + \int_{x_n}^{x_{n+1}} \left(\frac{x_{n+1} - x'}{\Delta} \right) * \frac{1}{\sqrt{(x_m - x')^2 + a^2}} \, dx' \tag{17}$$

After performing the integrations of Eq. (17), the expression for the matrix element is as follows

$$\begin{aligned} L_{mn} = {} & \frac{x_{n+1}}{\Delta} * \left[\log \frac{\left(\sqrt{a^2 + (x_{n+1} - x_m)^2} + x_{n+1} - x_m \right)}{\left(\sqrt{a^2 + (x_n - x_m)^2} + x_n - x_m \right)} \right] \\ & - \frac{x_{n-1}}{\Delta} * \left[\log \frac{\left(\sqrt{a^2 + (x_n - x_m)^2} + x_n - x_m \right)}{\left(\sqrt{a^2 + (x_{n-1} - x_m)^2} + x_{n-1} - x_m \right)} \right] \\ & - \frac{1}{\Delta} * \left[\frac{x_m \sqrt{a^2 + (x_{n+1} - x_m)^2} \log \left(2 \left(\sqrt{a^2 + (x_{n+1} - x_m)^2} + x_{n+1} - x_m \right) \right) + a^2 + (x_{n+1} - x_m)^2}{\sqrt{a^2 + (x_{n+1} - x_m)^2}} \right] \\ & - \frac{1}{\Delta} * \left[\frac{x_m \sqrt{a^2 + (x_{n-1} - x_m)^2} \log \left(2 \left(\sqrt{a^2 + (x_{n-1} - x_m)^2} + x_{n-1} - x_m \right) \right) + a^2 + (x_{n-1} - x_m)^2}{\sqrt{a^2 + (x_{n-1} - x_m)^2}} \right] \\ & + \frac{2}{\Delta} * \left[\frac{x_m \sqrt{a^2 + (x_n - x_m)^2} \log \left(2 \left(\sqrt{a^2 + (x_n - x_m)^2} + x_n - x_m \right) \right) + a^2 + (x_n - x_m)^2}{\sqrt{a^2 + (x_n - x_m)^2}} \right] \end{aligned} \tag{18}$$

$$V_m = 4\pi\varepsilon * V \tag{19}$$

The capacitance of cylinder is evaluated using Eq. (10) and Eq. (11).

2.4. Triangular Function as Basis and Pulse Function as Testing Functions

For this set of basis and testing functions, the expression as given by Eq. (19) is integrated considering the pulse testing function and replacing x_m of Eq. (19) by variable x over which the integration is carried out and the expression for the matrix element is given as follows:

$$\begin{aligned} L_{mn} &= \frac{x_{n+1}}{\Delta}(A_{1mn} - A_{2mn}) - \frac{x_{n-1}}{\Delta}(A_{2mn} - A_{3mn}) \\ &\quad -\frac{1}{\Delta}A_{4mn} - \frac{1}{\Delta}A_{5mn} + \frac{2}{\Delta}A_{6mn} \end{aligned} \tag{20}$$

where the expression for A_{1mn}, A_{2mn}, A_{3mn}, A_{4mn}, A_{5mn} and A_{6mn} are given as below:

$$\begin{aligned} A_{1mn} &= \sqrt{a^2+(x_{m+1}-x_{n+1})^2} - \sqrt{a^2+(x_{m-1}-x_{n+1})^2} \\ &\quad +\log\left[\frac{(\sqrt{a^2+(x_{m+1}-x_{n+1})^2} - x_{m+1}+x_{n+1})^{(x_{m+1}-x_{n+1})}}{(\sqrt{a^2+(x_{m-1}-x_{n+1})^2} - x_{m-1}+x_{n+1})^{(x_{m-1}-x_{n+1})}}\right] \end{aligned} \tag{21}$$

$$\begin{aligned} A_{2mn} &= \sqrt{a^2+(x_{m+1}-x_n)^2} - \sqrt{a^2+(x_{m-1}-x_n)^2} \\ &\quad +\log\left[\frac{(\sqrt{a^2+(x_{m+1}-x_n)^2} - x_{m+1}+x_n)^{(x_{m+1}-x_n)}}{(\sqrt{a^2+(x_{m-1}-x_n)^2} - x_{m-1}+x_n)^{(x_{m-1}-x_n)}}\right] \end{aligned} \tag{22}$$

$$\begin{aligned} A_{3mn} &= \sqrt{a^2+(x_{m+1}-x_{n-1})^2} - \sqrt{a^2+(x_{m-1}-x_{n-1})^2} \\ &\quad +\log\left[\frac{(\sqrt{a^2+(x_{m+1}-x_{n-1})^2} - x_{m+1}+x_{n-1})^{(x_{m+1}-x_{n-1})}}{(\sqrt{a^2+(x_{m-1}-x_{n-1})^2} - x_{m-1}+x_{n-1})^{(x_{m-1}-x_{n-1})}}\right] \end{aligned} \tag{23}$$

$$\begin{aligned} A_{4mn} &= \frac{1}{2}\log\left[\frac{\left(\sqrt{a^2+(x_{m+1}-x_{n+1})^2} - x_{m+1}+x_{n+1}\right)^{\left(x_{m+1}^2-x_{n+1}^2\right)}}{\left(\sqrt{a^2+(x_{m-1}-x_{n+1})^2} - x_{m-1}+x_{n+1}\right)^{\left(x_{m-1}^2-x_{n+1}^2\right)}}\right] \\ &\quad +\frac{1}{4}(3x_{m+1}+x_{n+1})\left(\sqrt{a^2+(x_{m+1}-x_{n+1})^2}\right) \\ &\quad -\frac{1}{4}(3x_{m-1}+x_{n+1})\left(\sqrt{a^2+(x_{m-1}-x_{n+1})^2}\right) \\ &\quad +\frac{a^2}{4}\log\left[\frac{(\sqrt{a^2+(x_{m+1}-x_{n+1})^2} + x_{m+1}-x_{n+1})}{(\sqrt{a^2+(x_{m-1}-x_{n+1})^2} + x_{m-1}-x_{n+1})}\right] \end{aligned} \tag{24}$$

$$A_{5mn} = \frac{1}{2}\log\left[\frac{\left(\sqrt{a^2+(x_{m+1}-x_{n-1})^2} - x_{m+1}+x_{n-1}\right)^{\left(x_{m+1}^2-x_{n-1}^2\right)}}{\left(\sqrt{a^2+(x_{m-1}-x_{n-1})^2} - x_{m-1}+x_{n-1}\right)^{\left(x_{m-1}^2-x_{n-1}^2\right)}}\right]$$

$$+\frac{1}{4}(3x_{m+1}+x_{n-1})\left(\sqrt{a^2+(x_{m+1}-x_{n-1})^2}\right)$$
$$-\frac{1}{4}(3x_{m-1}+x_{n-1})(\sqrt{a^2+(x_{m-1}-x_{n-1})^2})$$
$$+\frac{a^2}{4}\log\left[\frac{(\sqrt{a^2+(x_{m+1}-x_{n-1})^2}+x_{m+1}-x_{n-1})}{(\sqrt{a^2+(x_{m-1}-x_{n-1})^2}+x_{m-1}-x_{n-1})}\right] \quad (25)$$

$$A_{6mn}=\frac{1}{2}\log\left[\frac{\left(\sqrt{a^2+(x_{m+1}-x_n)^2}-x_{m+1}+x_n\right)^{\left(x_{m+1}^2-x_n^2\right)}}{\left(\sqrt{a^2+(x_{m-1}-x_n)^2}-x_{m-1}+x_n\right)^{\left(x_{m-1}^2-x_n^2\right)}}\right]$$
$$+\frac{1}{4}(3x_{m+1}+x_n)\left(\sqrt{a^2+(x_{m+1}-x_n)^2}\right)$$
$$-\frac{1}{4}(3x_{m-1}+x_n)\left(\sqrt{a^2+(x_{m-1}-x_n)^2}\right)$$
$$+\frac{a^2}{4}\log\left[\frac{\left(\sqrt{a^2+(x_{m+1}-x_n)^2}+x_{m+1}-x_n\right)}{\left(\sqrt{a^2+(x_{m-1}-x_n)^2}+x_{m-1}-x_n\right)}\right] \quad (26)$$

In the Eqs. (22) to (27) values of x_{m+1} and x_{m-1},

$$x_{m+1}=x_m+\frac{\Delta}{2}, \qquad x_{m-1}=x_m-\frac{\Delta}{2} \quad (27)$$

The expression for the elements of the excitation matrix is as follows

$$V_m=4\pi\varepsilon*\Delta*V \quad (28)$$

Using Eqs. (10) & (11), the capacitance and charge distribution are found.

2.5. Triangular Function Basis with Galerkin Weighting

For this case, the matrix elements L_{mn} are given by Eq. (6):

$$L_{mn}=\int_{x_{n-1}}^{x_n}\int_{x_{m-1}}^{x_m}\left(\frac{x'-x_{n-1}}{\Delta}\right)\left(\frac{x-x_{m-1}}{\Delta}\right)\frac{dx'dx}{\sqrt{a^2+(x-x')^2}}$$
$$+\int_{x_n}^{x_{n+1}}\int_{x_m}^{x_{m+1}}\left(\frac{x_{n+1}-x'}{\Delta}\right)\left(\frac{x_{m+1}-x}{\Delta}\right)\frac{dx'dx}{\sqrt{a^2+(x-x')^2}} \quad (29)$$

The integration result of Eq. (29) is as follows:

$$L_{mn} = A_{mn} - B_{mn} - C_{mn} + D_{mn} \tag{30}$$

where $A_{mn}, B_{mn}, C_{mn}, D_{mn}$ are given as follows,

$$\begin{aligned} A_{mn} &= \frac{x_{n+1}}{\Delta^2}\left(A_{1mn} - A_{2mn}\right) - \frac{x_{n-1}}{\Delta^2}\left(A_{2mn} - A_{3mn}\right) \\ &\quad -\frac{1}{\Delta^2}A_{4mn} - \frac{1}{\Delta^2}A_{5mn} + \frac{2}{\Delta^2}A_{6mn} \end{aligned} \tag{31}$$

$$\begin{aligned} A_{1mn} = &\frac{1}{4}\left(x_m + 3x_{n+1}\right)\sqrt{a^2 + \left(x_m - x_{n+1}\right)^2} \\ &-\frac{1}{4}a^2 \log\left(\frac{\left(\sqrt{a^2+\left(x_m-x_{n+1}\right)^2}+x_m-x_{n+1}\right)}{\left(\sqrt{a^2+\left(x_{m-1}-x_{n+1}\right)^2}+x_{m-1}-x_{n+1}\right)}\right) \\ &+\frac{1}{2}\left(x_m^2-x_{n+1}^2\right)\log\left(\sqrt{a^2+\left(x_m-x_{n+1}\right)^2}-x_m+x_{n+1}\right) \\ &-\frac{1}{4}\left(x_{m-1} + 3x_{n+1}\right)\sqrt{a^2 + \left(x_{m-1} - x_{n+1}\right)^2} \\ &-\frac{1}{2}\left(x_{m-1}^2-x_{n+1}^2\right)\log\left(\sqrt{a^2+\left(x_{m-1}-x_{n+1}\right)^2}-x_{m-1}+x_{n+1}\right) \end{aligned} \tag{32}$$

$$\begin{aligned} A_{2mn} &= \frac{1}{4}\left(x_m + 3x_n\right)\sqrt{a^2 + \left(x_m - x_n\right)^2} \\ &\quad -\frac{1}{4}a^2 \log\left(\frac{\left(\sqrt{a^2 + \left(x_m - x_n\right)^2} + x_m - x_n\right)}{\left(\sqrt{a^2 + \left(x_{m-1} - x_n\right)^2} + x_{m-1} - x_n\right)}\right) \\ &\quad +\frac{1}{2}\left(x_m^2 - x_n^2\right)\log\left(\sqrt{a^2 + \left(x_m - x_n\right)^2} - x_m + x_n\right) \\ &\quad -\frac{1}{4}\left(x_{m-1} + 3x_n\right)\sqrt{a^2 + \left(x_{m-1} - x_n\right)^2} \\ &\quad -\frac{1}{2}\left(x_{m-1}^2-x_n^2\right)\log\left(\sqrt{a^2+\left(x_{m-1}-x_n\right)^2}-x_{m-1}+x_n\right) \end{aligned} \tag{33}$$

$$\begin{aligned} A_{3mn} &= \frac{1}{4}\left(x_m + 3x_{n-1}\right)\sqrt{a^2 + \left(x_m - x_{n-1}\right)^2} \\ &\quad -\frac{1}{4}a^2 \log\left(\frac{\left(\sqrt{a^2 + \left(x_m - x_{n-1}\right)^2} + x_m - x_{n-1}\right)}{\left(\sqrt{a^2 + \left(x_{m-1} - x_{n-1}\right)^2} + x_{m-1} - x_{n-1}\right)}\right) \end{aligned}$$

$$+\frac{1}{2}\left(x_m^2-x_{n-1}^2\right)\log\left(\sqrt{a^2+\left(x_m-x_{n-1}\right)^2}-x_m+x_{n-1}\right)$$
$$-\frac{1}{4}\left(x_{m-1}+3x_{n-1}\right)\sqrt{a^2+\left(x_{m-1}-x_{n-1}\right)^2}$$
$$-\frac{1}{2}\left(x_{m-1}^2-x_{n-1}^2\right)\log\left(\sqrt{a^2+\left(x_{m-1}-x_{n-1}\right)^2}-x_{m-1}+x_{n-1}\right) \quad (34)$$

$$A_{4mn}=\frac{1}{3}\log\left[\frac{\left(\sqrt{a^2+\left(x_m-x_{n+1}\right)^2}-x_m+x_{n+1}\right)^{\left(x_m^3-x_{n+1}^3\right)}}{\left(\sqrt{a^2+\left(x_{m-1}-x_{n+1}\right)^2}-x_{m-1}+x_{n+1}\right)^{\left(x_{m-1}^3-x_{n+1}^3\right)}}\right]$$
$$+\frac{1}{9}\sqrt{a^2+\left(x_m-x_{n+1}\right)^2}\left(a^2+4x_m^2+x_mx_{n+1}+4x_{n+1}^2\right)$$
$$-\frac{1}{9}\sqrt{a^2+\left(x_{m-1}-x_{n+1}\right)^2}\left(a^2+4x_{m-1}^2+x_{m-1}x_{n+1}+4x_{n+1}^2\right) \quad (35)$$

$$A_{5mn}=\frac{1}{3}\log\left[\frac{\left(\sqrt{a^2+\left(x_m-x_{n-1}\right)^2}-x_m+x_{n-1}\right)^{\left(x_m^3-x_{n-1}^3\right)}}{\left(\sqrt{a^2+\left(x_{m-1}-x_{n-1}\right)^2}-x_{m-1}+x_{n-1}\right)^{\left(x_{m-1}^3-x_{n-1}^3\right)}}\right]$$
$$+\frac{1}{9}\sqrt{a^2+\left(x_m-x_{n-1}\right)^2}\left(a^2+4x_m^2+x_mx_{n-1}+4x_{n-1}^2\right)$$
$$-\frac{1}{9}\sqrt{a^2+\left(x_{m-1}-x_{n-1}\right)^2}\left(a^2+4x_m^2+x_{m-1}x_{n-1}+4x_{n-1}^2\right) \quad (36)$$

$$A_{6mn}=\frac{1}{3}\log\left[\frac{\left(\sqrt{a^2+\left(x_m-x_n\right)^2}-x_m+x_n\right)^{\left(x_m^3-x_n^3\right)}}{\left(\sqrt{a^2+\left(x_{m-1}-x_n\right)^2}-x_{m-1}+x_n\right)^{\left(x_{m-1}^3-x_n^3\right)}}\right]$$
$$+\frac{1}{9}\sqrt{a^2+\left(x_m-x_n\right)^2}\left(a^2+4x_m^2+x_mx_n+4x_n^2\right)$$
$$-\frac{1}{9}\sqrt{a^2+\left(x_{m-1}-x_n\right)^2}\left(a^2+4x_{m-1}^2+x_{m-1}x_n+4x_n^2\right) \quad (37)$$

In order to find the expression for the second term B_{mn} in Eq. (30), integration is carried out with limit is x_m to x_{m+1} instead of x_{m-1} to x_m as used for finding the terms for the first term that A_{mn}. Let

us consider these equations are B_{1mn} to B_{6mn} than final integration results,

$$\begin{aligned} B_{mn} &= \frac{x_{n+1}}{\Delta^2}(B_{1mn} - B_{2mn}) - \frac{x_{n-1}}{\Delta^2}(B_{2mn} - B_{3mn}) \\ &\quad -\frac{1}{\Delta^2}B_{4mn} - \frac{1}{\Delta^2}B_{5mn} + \frac{2}{\Delta^2}B_{6mn} \end{aligned} \tag{38}$$

On carrying out the integration, the third term C_{mn} in Eq. (30) gives,

$$\begin{aligned} C_{mn} &= \frac{x_{m-1}x_{n+1}}{\Delta^2}(C_{1mn} - C_{2mn}) - \frac{x_{m-1}x_{n-1}}{\Delta^2}(C_{2mn} - C_{3mn}) \\ &\quad -\frac{x_{m-1}}{\Delta^2}C_{4mn} - \frac{x_{m-1}}{\Delta^2}C_{5mn} + \frac{2x_{m-1}}{\Delta^2}C_{6mn} \end{aligned} \tag{39}$$

$$\begin{aligned} C_{1mn} &= \sqrt{a^2 + (x_m - x_{n+1})^2} - \sqrt{a^2 + (x_{m-1} - x_{n+1})^2} \\ &\quad +\log\left[\frac{\left(\sqrt{a^2+(x_m-x_{n+1})^2}-x_m + x_{n+1}\right)^{(x_m-x_{n+1})}}{\left(\sqrt{a^2+(x_{m-1}-x_{n+1})^2}-x_{m-1}+x_{n+1}\right)^{(x_{m-1}-x_{n+1})}}\right] \end{aligned} \tag{40}$$

$$\begin{aligned} C_{2mn} &= \sqrt{a^2 + (x_m - x_n)^2} - \sqrt{a^2 + (x_{m-1} - x_n)^2} \\ &\quad +\log\left[\frac{(\sqrt{a^2 + (x_m - x_n)^2} - x_m + x_n)^{(x_m-x_n)}}{(\sqrt{a^2 + (x_{m-1} - x_n)^2} - x_{m-1} + x_n)^{(x_{m-1}-x_n)}}\right] \end{aligned} \tag{41}$$

$$\begin{aligned} C_{3mn} &= \sqrt{a^2 + (x_m - x_{n-1})^2} - \sqrt{a^2 + (x_{m-1} - x_{n-1})^2} \\ &\quad +\log\left[\frac{\left(\sqrt{a^2+(x_m-x_{n-1})^2}-x_m+x_{n-1}\right)^{(x_m-x_{n-1})}}{\left(\sqrt{a^2+(x_{m-1}-x_{n-1})^2}-x_{m-1}+x_{n-1}\right)^{(x_{m-1}-x_{n-1})}}\right] \end{aligned} \tag{42}$$

$$\begin{aligned} C_{4mn} &= \frac{1}{2}\log\left[\frac{\left(\sqrt{a^2+(x_m-x_{n+1})^2}-x_m+x_{n+1}\right)^{(x_m^2-x_{n+1}^2)}}{\left(\sqrt{a^2+(x_{m-1}-x_{n+1})^2}-x_{m-1}+x_{n+1}\right)^{(x_{m-1}^2-x_{n+1}^2)}}\right] \\ &\quad +\frac{1}{4}(3x_m + x_{n+1})\sqrt{a^2 + (x_m - x_{n+1})^2} \\ &\quad -\frac{1}{4}(3x_{m-1} + x_{n+1})\sqrt{a^2 + (x_{m-1} - x_{n+1})^2} \\ &\quad +\frac{a^2}{4}\log\left[\frac{\left(\sqrt{a^2 + (x_m - x_{n+1})^2} + x_m - x_{n+1}\right)}{\left(\sqrt{a^2 + (x_{m-1} - x_{n+1})^2} + x_{m-1} - x_{n+1}\right)}\right] \end{aligned} \tag{43}$$

$$C_{5mn} = \frac{1}{2}\log\left[\frac{\left(\sqrt{a^2+(x_m-x_{n-1})^2}-x_m+x_{n-1}\right)^{(x_m^2-x_{n-1}^2)}}{\left(\sqrt{a^2+(x_{m-1}-x_{n-1})^2}-x_{m-1}+x_{n-1}\right)^{\left(x_{m-1}^2-x_{n-1}^2\right)}}\right]$$
$$+\frac{1}{4}(3x_m+x_{n-1})\sqrt{a^2+(x_m-x_{n-1})^2}$$
$$-\frac{1}{4}(3x_{m-1}+x_{n-1})\sqrt{a^2+(x_{m-1}-x_{n-1})^2}$$
$$+\frac{a^2}{4}\log\left[\frac{\left(\sqrt{a^2+(x_m-x_{n-1})^2}+x_m-x_{n-1}\right)}{\left(\sqrt{a^2+(x_{m-1}-x_{n-1})^2}+x_{m-1}-x_{n-1}\right)}\right] \quad (44)$$

$$C_{6mn} = \frac{1}{2}\log\left[\frac{(\sqrt{a^2+(x_m-x_n)^2}-x_m+x_n)^{(x_m^2-x_n^2)}}{(\sqrt{a^2+(x_{m-1}-x_n)^2}-x_{m-1}+x_n)^{(x_{m-1}^2-x_n^2)}}\right]$$
$$+\frac{1}{4}(3x_m+x_n)\sqrt{a^2+(x_m-x_n)^2}$$
$$-\frac{1}{4}(3x_{m-1}+x_n)\sqrt{a^2+(x_{m-1}-x_n)^2}$$
$$+\frac{a^2}{4}\log\left[\frac{\left(\sqrt{a^2+(x_m-x_n)^2}+x_m-x_n\right)}{\left(\sqrt{a^2+(x_{m-1}-x_n)^2}+x_{m-1}-x_n\right)}\right] \quad (45)$$

In order to find out the last term of Eq. (30), similar expressions are obtained as in Eqs. (38)–(44) by replacing integration limit by x_m *to* x_{m+1} instead of x_{m-1} *to* x_m. The expression of the term D_{mn} is as follows:

$$D_{mn} = \frac{x_{m-1}x_{n+1}}{\Delta^2}(D_{1mn}-D_{2mn})-\frac{x_{m-1}x_{n-1}}{\Delta^2}(D_{2mn}-D_{3mn})$$
$$-\frac{x_{m+1}}{\Delta^2}D_{4mn}-\frac{x_{m+1}}{\Delta^2}D_{5mn}+\frac{2x_{m+1}}{\Delta^2}D_{6mn} \quad (46)$$

The expression for the elements of the excitation matrix is given by

$$V_m = 4\pi\varepsilon * V * \left\{\int_{x_{m-1}}^{x_m}\left(\frac{x-x_{m-1}}{\Delta}\right)dx+\int_{x_m}^{x_{m+1}}\left(\frac{x_{m+1}-x}{\Delta}\right)dx\right\} \quad (47)$$

$$V_m = \frac{4\pi\varepsilon}{\Delta} * V * \left\{x_m^2-\frac{x_{m-1}^2}{2}-\frac{x_{m+1}^2}{2}-x_{m-1}(x_m-x_{m-1})\right.$$
$$\left.+x_{m+1}(x_{m+1}-x_m)\right\} \quad (48)$$

Using Eqs. (10) & (11), capacitance and charge density of metallic cylinder for this set basis and testing functions are evaluated.

Table 1. Comparison for capacitance of charged conducting cylinder.

Length(L)/ Diameter(d)	Capacitance/Unit Length (pF/m)			
	Analytical method	**Pulse-Delta Harrington**	**Pulse-Pulse**	**Triangular-Delta**
6	22.33	25.9	25.47	21.7
10	18.55	18.31	20.87	18.65
15	16.35	18.65	18.37	16.61
20	15.08	16.7	16.86	15.4
25	14.22	15.56	15.79	14.52
30	13.59	14.77	15.00	13.89
60	11.62	12.4	12.58	11.90

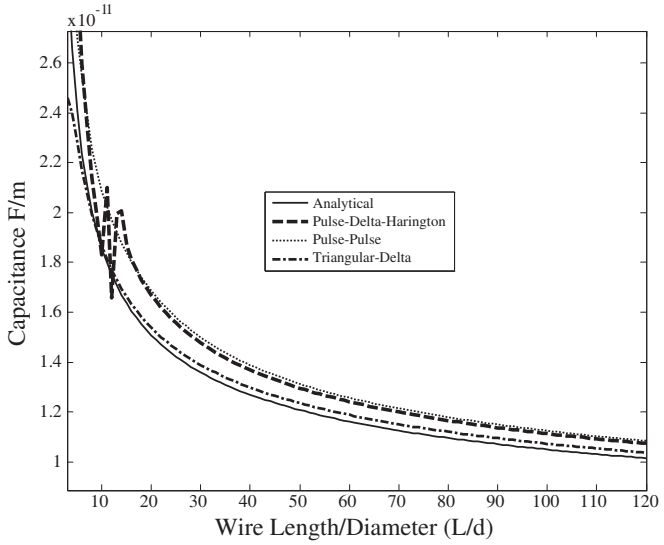

Figure 4. Variation of capacitance of hollow cylinder with height by diameter ratio using present method and analytical method.

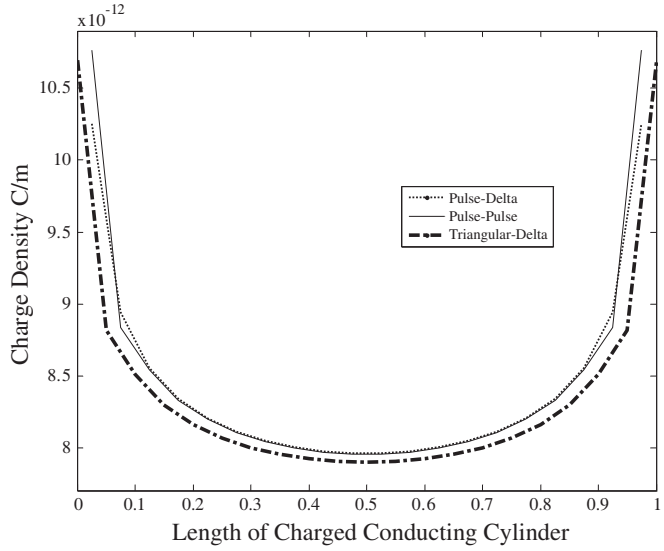

Figure 5. Charge distribution of conducting cylinder for different basis and testing function with number of subsections $N = 10$.

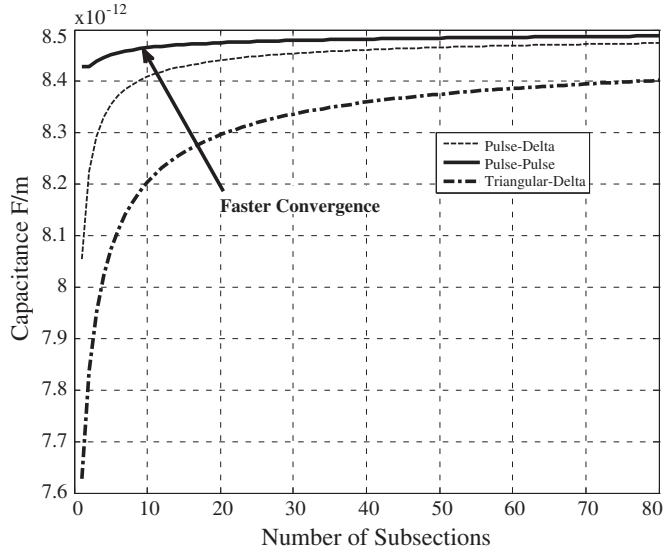

Figure 6. Capacitance per unit length of charged conducting cylinder as a function of number of subsections with simulation parameter length/diameter = 500.

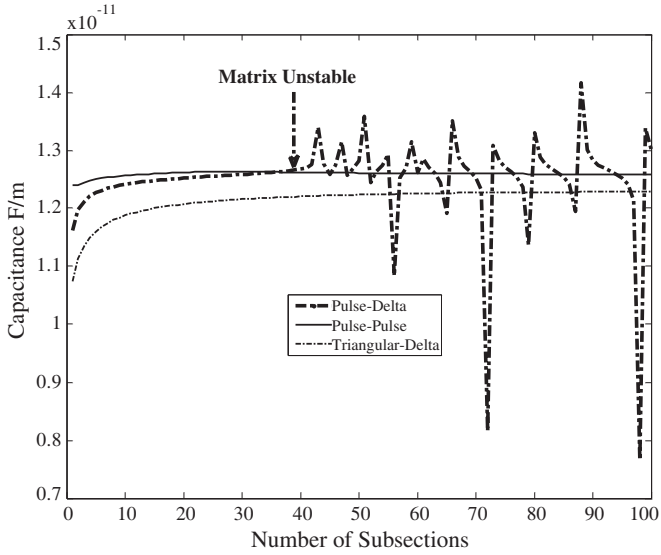

Figure 7. Capacitance per unit length of charged conducting cylinder as a function of number of subsections with simulation parameter cylinder length/diameter = 60.

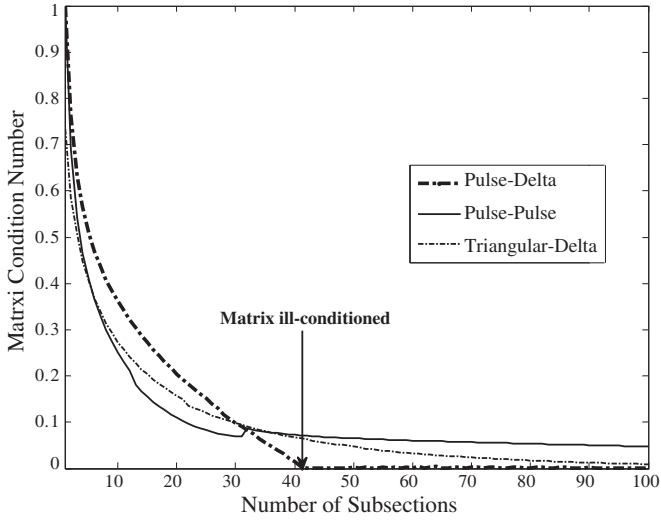

Figure 8. Matrix condition number as a function of number of subsections with simulation parameter cylinder length/diameter = 60.

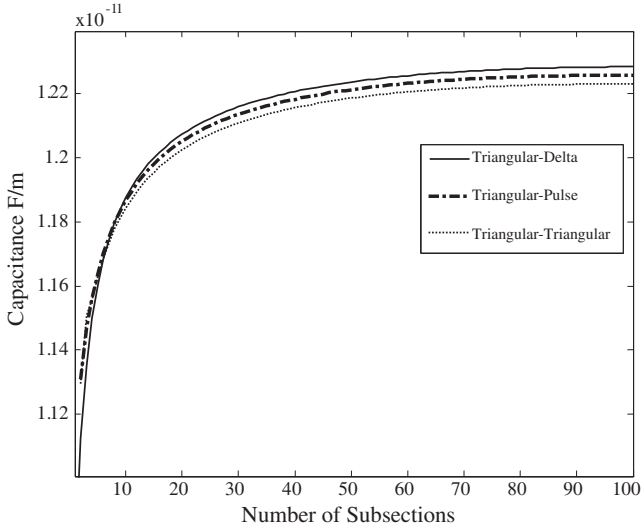

Figure 9. Capacitance per unit length of charged conducting cylinder as a function of number of subsections for triangular basis function and different testing function with $L/d = 60$.

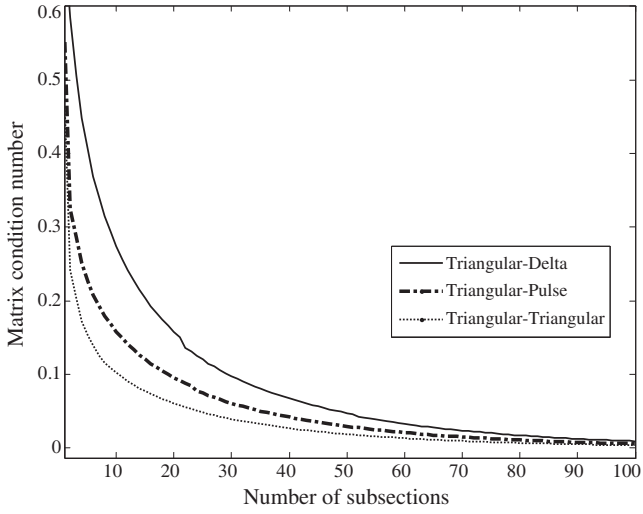

Figure 10. Matrix condition number as a function of number of subsections for triangular basis function and different testing function with $L/d = 60$.

3. NUMERICAL RESULTS

The matrix elements are computed using the expressions of L_{mn} for different basis and testing functions sets as given by Eqs. (9), (14), (18), (20)–(27), (29)–(46) for pulse/delta, pulse/pulse, triangle/delta, triangle/pulse, triangle/triangle basis/testing function sets respectively. After the matrix is formed, it is inverted and the inverted matrix is multiplied by the excitation voltage matrix to find the unknown charge distribution on each subsections. Substituting the value of charge density from Eq. (10) and the basis function from Eq. (7) or Eq. (15) into Eq. (11), the total charge and the capacitance of the charged conducting cylinder is obtained.

The data on capacitance computed using different basis and a testing function set are compared with that of the methods of Harrington [1] & analytical method [5], and is presented in Table 1. The values of the capacitance are also computed for different value of radius and are presented in Fig. 4.

Using expressions for matrix elements, the capacitance per unit length of the conducting cylinder for different basis and testing functions is evaluated with different value of cylinder radius. The convergence of the numerical data on the capacitance per unit length is checked for different basis and testing functions. Fig. 5 shows the charge density on a charged conducting cylinder of length to diameter ration 500. In order to illustrate the convergence properties, the charge density was computed using pulse and triangular basis functions with the same number of subsection, $N = 10$.

The convergence of the numerical data on the capacitance per unit length is checked for each different case. The convergence data is presented in Fig. 6. The convergence data on capacitance for the length/diameter ratio 60 has been depicted in Fig. 7.

Figure 8 shows the effect in matrix condition number with increasing the number of subsections for different basis and testing function. The condition number of a matrix measures the sensitivity of the solution of a system of linear equations to errors in the data. The greater the condition numbers of a linear system, the more sensitive the equations to slight perturbations and the more numerical error likely to appear in the solution. If matrix L_{mn} is well conditioned, rcond (L_{mn}) is near 1.0. If L_{mn} is badly conditioned, rcond (L_{mn}) is near 0.0.

For similar simulation parameters, the convergence data for triangular basis function and different kinds of testing functions is presented in Fig. 9 and the corresponding values of matrix condition number is presented in Fig. 10.

4. CONCLUSION

The results in Fig. 4 shows that the capacitance value computed using triangular basis and delta testing function have faster convergence of capacitance and match very well with analytical result which is exact. For the lower value of h/d (ranging from 5 to 15), instability in the numerical value of capacitance for the case of pulse basis and delta testing function has also been observed. The free charge distribution on a metallic surface shoots up at the edges and is relatively flat at the middle portion of the conductor [2], which is the reason that the slope of the charge distribution is steeper as the edge of the conductor is approached, and thus the rate of increase of charge density is more as one approaches the edges of the conductor as shown in Fig. 5. For a smooth curve of charge density with axial distance of the conducting cylinder, the number of sub-sections should be very large to approximate the sharp rise in charge distribution. The jagged line in Fig. 5 will be removed if the number of sections is increased beyond this convergence criterion but in that case the matrix may become ill-conditioned. The convergence data in Fig. 6 shows that the pulse basis with Galerkin weighting converges faster than method of Harrington [1] as the number of segments N increases for a small cylinder radius.

Figure 7 depicts the value of numerical capacitance as a function of the number of segments for cylinder length to diameter ratio 60. As the radius increases, instability in the value of capacitance for pulse basis and delta testing method is observed. Fig. 8 shows the dependence of the condition number of L_{mn} matrix on the number of segments. It is noted that the co-efficient matrix is relatively well conditioned when triangular basis function and delta function as testing function is used in the method of moment. Similar studies were carried out using triangular basis function for pulse as well as triangular testing (Galerkin weighting). But in those cases the calculation of matrix elements L_{mn} is relatively more complex and no significance improvement is achieved in the convergence. Hence, the triangular basis and delta testing method is considered optimum.

ACKNOWLEDGMENT

The first author thanks the Vice Chancellor of Dharmsinh Desai University for his support & encouragement. The authors also express gratitude to Dr. Nikhil Kothari for his personal support in terms of providing the required environment & facilities to carry out this work.

REFERENCES

1. Harrington, R. F., *Field Computation by Method of Moment*, Macmillan, New York, 1968.
2. Gibson, W. C., *The Method of Moments in Electromagnetics*, Chapman & Hall/CRC, Taylor & Francis Group, 2008.
3. Das, B. N. and S. B. Chakrabarty, "Capacitance and charge distribution of two cylindrical conductors of finite length," *IEE Proceedings of Measurement Technology*, Vol. 144, No. 6, 280–286, 1997.
4. Das, B. N. and S. B. Chakrabarty, "Calculation of the electrical capacitance of a truncated cone," *IEEE Transactions of Electromagnetic Compatibility*, Vol. 39, No. 4, 371–374, 1997.
5. Chakraborty, C., D. R. Poddar, A. Chakraborty, and B. N. Das, "Electrostatic charge distribution and capacitance of isolated cylinders and truncated cones in free space," *IEEE Transactions on Electromagnetic Compatibility*, Vol. 35, No. 1, February 1993.
6. Das, B. N. and S. B. Chakrabarty, "Capacitance of metallic structures in the form of paraboloidal and spherical reflectors," *IEEE Transactions of Electromagnetic Compatibility*, Vol. 39, No. 4, 390–393, 1997.
7. Ghosh, S. and A. Chakrabarty, "Estimation of capacitance of different conducting bodies by the method of rectangular subareas," *Journal of Electrostatics*, Vol. 66, 142–146, 2008.
8. Das, B. N. and S. B. Chakrabarty, "Evaluation of capacitance and charge distribution of cylinder of finite length with top and bottom cover plates," *Indian Journal of Radio & Space Physics*, Vol. 26, 112–115, 1997.
9. Prarthan D. M. and S. B. Chakrabarty, "Capacitance of dielectric coated metallic bodies isolated in free space," *Electromagnetics*, Vol. 31, No. 4, 294–314, 2011.
10. Das, B. N. and S. B. Chakrabarty, "Rigorous analysis of the effect of dielectric coating on metallic bodies isolated in free space," *Proceedings of INSA-A*, Vol. 64-A-2, 137–148, 1998.
11. Chakrabarty, S. B., S. Das, and B. N. Das, "Capacitance of dielectric coated cylinder of finite axial length and truncated cone isolated in free space," *IEEE Transactions on Electromagnetic Compatibility*, Vol. 44, No. 2, 394-398, 2002.
12. Wheless, W. and L. T. Wartz, "Introducing undergraduates to the moment method," *IEEE Transactions on Education Introducing Undergraduates to the Moment Method*, Vol. 38, No. 4, November 1995.

13. Ouda, M., "Efficient capacitance matrix computation of large conducting bodies using the characteristic basis function method," *Journal of Applied Sciences*, Vol. 10, No. 15, 1622–1626, 2010.